LA-UR-15-20835
Approved for public release; distribution is unlimited.

Title: Observation of cyclotron resonance and electron-phonon coupling in surface states of the bulk-insulating topological insulator Cu0:02Bi2Se3

Author(s): Wu, Liang
Tse, Wang-Kong
Morris, C. M.
Brahlek, M.
Koirala, N.
Oh, S.
Armitage, N. P.

Intended for: Journal Physical Review Letters and Arxiv

Issued: 2015-02-05

Observation of cyclotron resonance and electron-phonon coupling in surface states of the bulk-insulating topological insulator $Cu_{0.02}Bi_2Se_3$

Liang Wu,[1] Wang-Kong Tse,[2] C. M. Morris,[1] M. Brahlek,[3] N. Koirala,[3] S. Oh,[3] and N.P. Armitage[1,*]

[1]*The Institute for Quantum Matter, Department of Physics and Astronomy, The Johns Hopkins University, Baltimore, MD 21218 USA.*

[2]*Los Alamos National Laboratory, Los Alamos, NM 87545, USA*

[3]*Department of Physics and Astronomy, Rutgers the State University of New Jersey. Piscataway, NJ 08854*

(Dated: January 26, 2015)

We have utilized magneto-optical time-domain spectroscopy to investigate the low frequency optical response of topological insulator $Cu_{0.02}Bi_2Se_3$ and Bi_2Se_3 films. With both field and frequency depedence, such experiments give sufficient information to measure the mobility and carrier density of multiple conduction channels simultaneously. We observe sharp cyclotron resonances (CRs) in both samples. The small amount of Cu substitution into the $Cu_{0.02}Bi_2Se_3$ induces a true bulk insulator with only a single conduction channel with total sheet carrier density $\sim 4.9\times10^{12}/\mathrm{cm}^2$ and mobility as large as 4000 $\mathrm{cm}^2/\mathrm{V{\cdot}s}$. This is consistent with pure topological surface state (TSSs) conduction with a chemical potential ~150 meV above the Dirac point. Hence, a true topological insulator with an insulating bulk is realized. The CR broadens at high fields, an effect that we attribute to an electron-phonon interaction. This assignment is supported by an extended Drude model analysis on the zero field data. In contrast to $Cu_{0.02}Bi_2Se_3$, two charge channels were observed in normal Bi_2Se_3 films. We demonstrate a method to distinguish between the dominant TSSs and trivial bulk/2DEG states. The dominant channel exhibits a CR with a carrier density of $\sim 2.0\times10^{13}/\mathrm{cm}^2$ and mobility $\sim$ 3200 $\mathrm{cm}^2/\mathrm{V{\cdot}s}$, consistent with TSSs with a chemical potential $\sim$ 350meV above the Dirac point.

Topological insulators (TIs) are a newly discovered class of materials characterized by an inverted band structure [1–3] caused by strong spin-orbit coupling. In the ideal case, they have an insulating bulk and only conduct via massless Dirac topological surface states (TSSs). Spin-momentum locking in their electronic structure makes TIs a promising platforms for spintronics applications [4]. Progress in this field has been hampered by the fact that all discovered TIs to date are slightly doped and have a conducting bulk. For instance, exotic $p+ip$ interface superconductivity between a bulk-insulating TI and an s-wave superconductor was predicted to exist, but has been not definitively confirmed due to residual bulk conduction [5]. Axion electrodynamics [6] and quantized Faraday rotation [7] in units of the fine structure constant α ($\sim 0.4\,^\circ$) also remains unobserved. Moreover, a conducting bulk hinders the exploration of interaction effects in the TSSs because screening is strong at high carrier density. Tuning the chemical potential towards the Dirac point and enhancing mobility was shown to be very successful in probing many-body interactions in graphene [8]. Similar advancement is expected in TIs, but has not yet been realized.

The band structure of Bi_2Se_3 is one of the simplest of the 3D TIs with only a single Dirac cone at the center of the surface Brillouin zone. The possibility of high quality stoichiometric growth by MBE [9, 10] and a large 300meV gap makes room temperature applications plausible. Unfortunately, Bi_2Se_3 is known to have a conducting bulk due to defects from the growth process. Suppression of the bulk carrier density has been achieved by chemical doping methods [11–14]. Nevertheless, these samples still have significant densities of bulk carriers or impurity states that are pinned near E_F. Gating has also been used to deplete bulk carriers and enhance mobility [15, 16], but an external high voltage is not convenient for device applications. Recently it was found that $\sim$ 2% Cu doping suppressed the bulk carriers and a true insulating state was realized in thin films [17]. Here we investigate these copper doped bulk insulating thin films and their conducting surface states, outside of the superconducting regime investigated in some previous works[17].

Cyclotron resonance (CR) experiments are a powerful tool to study Dirac fermions and probe many-body interaction [18, 19]. CR is also one of the most accurate measures of effective mass [20]. In previous work, a large Kerr rotation in bulk-conducting Bi_2Se_3 films was claimed from CR of TSSs, but no sharp resonance feature was observed [21]. Cyclotron resonance has been reported in In_2Se_3 capped films [22], but large Indium diffusion from In_2Se_3 to Bi_2Se_3 [23] ruins the simple non-TI/TI boundary at the interface, as the topological phase transition occurs at low Indium concentrations ($\sim$ 6%) [24].

In the present work, we used magneto-optical time-domain terahertz spectroscopy with 'fast rotator' technique [25] to observe sharp cyclotron resonances in both $Cu_{0.02}Bi_2Se_3$ and pure Bi_2Se_3 thin films. We demonstrate that $Cu_{0.02}Bi_2Se_3$ can be described by a *single* Drude component with total carrier density $n_{2D} \sim 4.9\times10^{12}/\mathrm{cm}^2$. This Drude contribution is consistent with pure surface state transport with an $E_F \sim$ 150 meV above the Dirac point(70meV below the conduction band), which makes $Cu_{0.02}Bi_2Se_3$ a true topological insulator. This can be compared to Bi_2Se_3 where we found two channel conduction. Consistent with our previous work [21, 24], we determine that the large Faraday rotation (rotation of transmitted linearly polarized light) in this material is induced by a dominant high mobility channel with sheet carrier density $n_{2D} \sim 2.0\times10^{13}/\mathrm{cm}^2$, which is consistent with TSSs with an $E_F \sim$ 350meV. However, a subdominant low-mobility

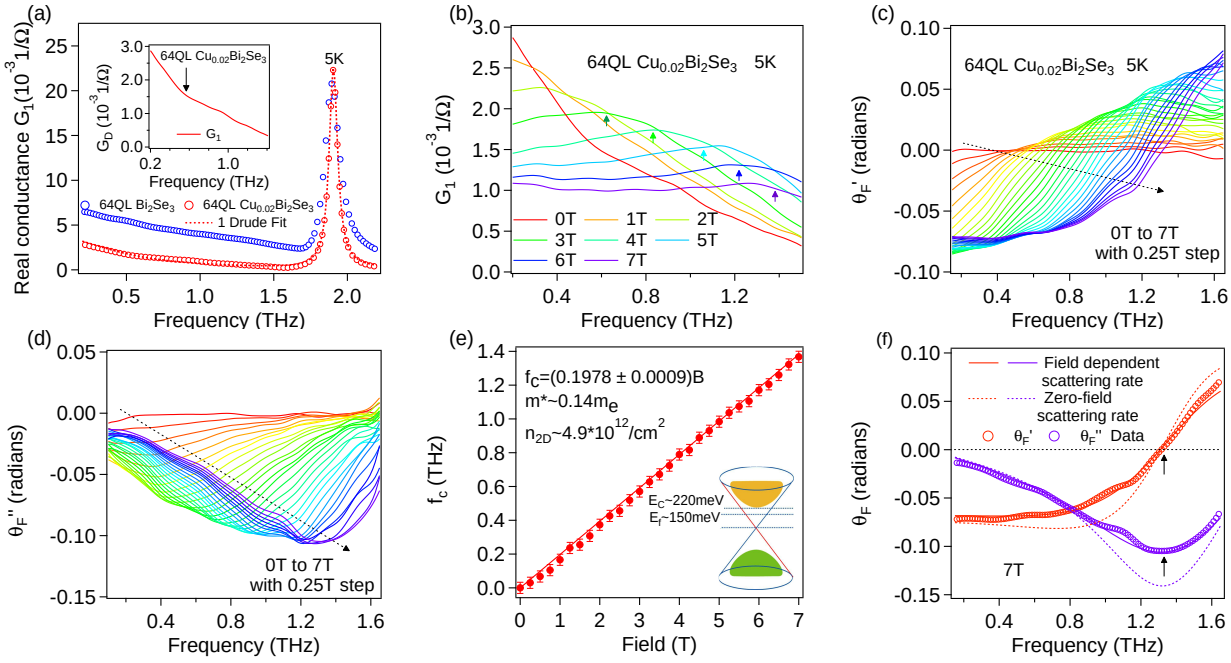

FIG. 1: (Color online) (a) Real sheet conductance of 64QL $Cu_{0.02}Bi_2Se_3$ and Bi_2Se_3 films at 5K. Inset is the Drude conductance G_D of 64QL $Cu_{0.02}Bi_2Se_3$ after subtracting the phonon and ϵ_∞ contributions. (b) Field dependent conductance of 64QL $Cu_{0.02}Bi_2Se_3$ film at 5K. Arrows are guides to the eye for cyclotron resonances. (c) Real and (d) Imaginary part of complex Faraday rotation data for 64QL $Cu_{0.02}Bi_2Se_3$ films at different fields at 5K. (e) Cyclotron frequency versus field. The inset is a cartoon indicating $E_F = 150meV$, 70mev below conduction band minimum. (f) Complex Faraday angle with fit at 7T. Solid curves are fits with variable scattering rate as a function of field. Dashed curves are fit using the zero-field scattering rate. Arrows are guides for cyclotron frequencies to the eye.

second Drude term is also required to fit the data. This subdominant term, which likely derives from trivial states (bulk and/or 2DEG) is featureless in the Faraday rotation and only gives a small flat background.

In Fig. 1(a), we show the zero field THz range conductance of a 64QL $Cu_{0.02}Bi_2Se_3$ film, as compared to 64QL Bi_2Se_3. The Cu substituted sample's spectra are characterized by a reduced total spectral weight and slightly lower scattering rate than the pure Bi_2Se_3. The spectra can be well fit by a Drude-Lorentz model with a Drude term describing free electron-like motion, a Drude-Lorentz term modeling the photon and a lattice polarizability ϵ_∞ term that originates from absorptions outside the spectral range.

$$G(\omega) = \left(-\frac{\omega_{pD}^2}{i\omega - \Gamma_D} - \frac{i\omega\omega_{pDL}^2}{\omega_{DL}^2 - \omega^2 - i\omega\Gamma_{DL}} - i\left(\epsilon_\infty - 1\right)\omega \right) \epsilon_0 d. \tag{1}$$

Here Γ's are scattering rates, ω_p's are plasma frequencies, and d is the film thickness. The spectral weight (ω_p^2) is proportional to the integrated area of each feature in the real part of the conductance. It gives the ratio of carrier density to an effective transport mass. Considering the TSS dispersion up to quadratic corrections, the spectral weight can be expressed in terms of k_F [24], where A and B are TSS dispersion parameters.

$$\frac{2}{\pi\epsilon_0}\int G_1 d\omega = \omega_p^2 d = \frac{n_{2D}e^2}{m^*\epsilon_0} = \frac{k_F(A + 2Bk_F)e^2}{2\pi\hbar^2\epsilon_0} \tag{2}$$

Lower spectral weight means lower carrier density and smaller effective mass (see supplementary information(SI)). From Drude-Lorentz fits, we find $\omega_p^2 d$ and obtain $E_F \sim 150$ meV, $m^* \sim 0.14m_e$ and a total sheet carrier density $n_{2D} \sim 5.0 \times 10^{12}/\mathrm{cm}^2$.

Above, we could estimate carrier density and mass by the zero field spectra alone because both can be expressed as a function of k_F. Below we determine the mass in a model free fashion through cyclotron resonance experiments. The signature of CR is a peak in the real part of the conductance (1(b)), an inflection point in real part of Faraday rotation (1(c)) and a dip in the imaginary part of Faraday rotation (1(d)), which shifts with magnetic field. Its full width at half maximum (FWHM) is the scattering rate. We use the fast rotato technique to measure the polarization states with resolution 0.5mrad [25] (See SI for experimental details). Field dependent complex Faraday rotation data are shown in Fig. 1(c)(d). One can see that an edge feature around an inflection point in the real part and a dip in the imaginary part shifts to higher frequency with increasing field, which is consistent with cyclotron resonance. We fit the data by a Drude-Lorentz model accounting for the field dependence for the Drude term and constraining the parameters of the phonon and the high-

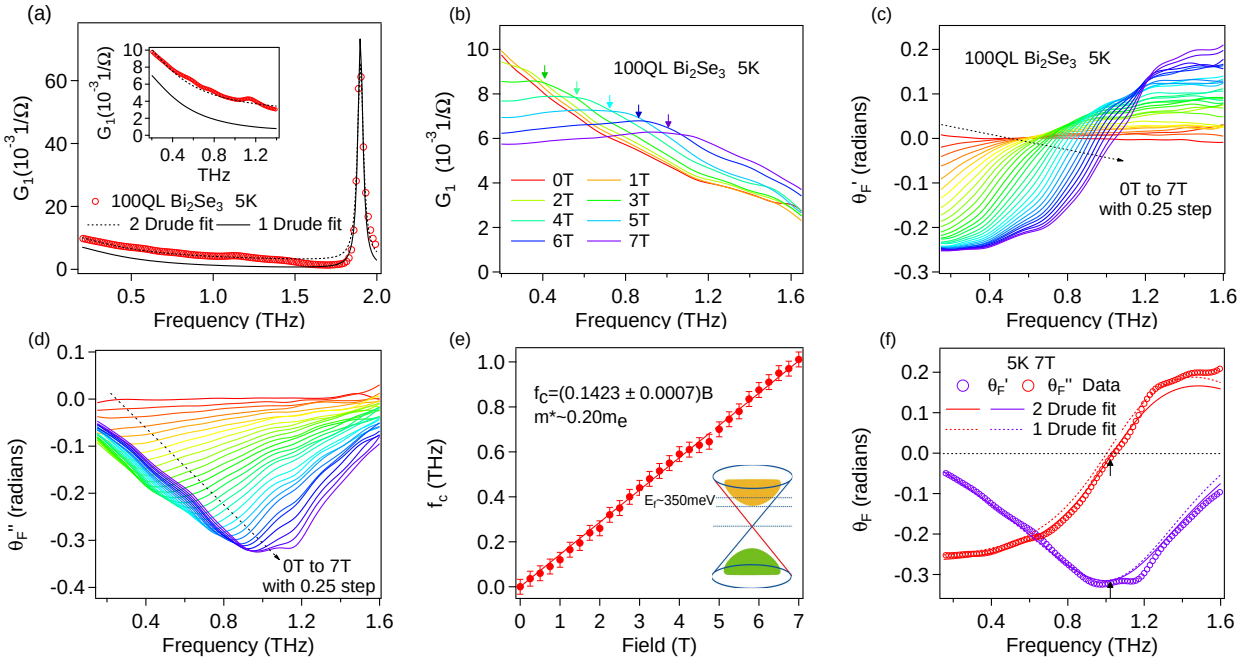

FIG. 2: (Color online) (a) Real conductance of 100QL Bi_2Se_3 comparing single and two component Drude fits. Inset enlarges the low frequency part. (b) Field dependent conductance 5K. (c) Real and (d) Imaginary part of complex Faraday rotation data at different fields at 5K. (e) Cyclotron resonance frequency versus field. The inset is a cartoon indicating E_F = 350 meV Dirac point. (f) Complex Faraday rotation data with fit at 7T. The solid curve is the two Drude fit. Dashed curve is one Drude fit.

frequency terms by values extracted from zero-field conductance. Conductance in a magnetic field is described by the expression.

$$G_{\pm} = -i\epsilon_0\omega d\Big[\frac{\omega_D^2}{-\omega^2 - i\Gamma_D\omega \mp \omega_c\omega} + \frac{\omega_{pDL}^2}{\omega_{DL}^2 - \omega^2 - i\omega\Gamma_{DL}} + (\epsilon_\infty - 1)\Big]. \quad (3)$$

Here the ± sign signifies the response to right/left-hand circularly polarized light, respectively, and ω_c is the cyclotron frequency to be defined below. The transmission can be analyzed according the thin film transmission equation [26] for each polarization handedness separately. The Faraday rotation can be then expressed as $\tan(\theta_F) = -i(t_+ - t_-)/(t_+ + t_-)$ where $t_\pm$ is the transmission for right/left-hand circularly polarized light. Note that the Faraday equation is a complex quantity because in addition to rotations, phase shifts that are different for right/left hand polarized light can be accumulated. The imaginary part is related to the ellipticity [25].

The fits to this model for the Faraday rotation are shown for a representative field of 7T in Fig. 1(f) (see SI for fits to all fields). In this plot the dashed curves are fits with fixed spectral weight and scattering rate ~ 0.4THz (obtained from the zero-field conductance fit). One can see that although the gross features of the spectra are reproduced, using the parameters of the zero field spectra in their entirety fails to reproduce certain aspects of the Faraday rotation, including its maximum. A much better fit (solid line) can be reached by letting the scattering rate vary with field, while keeping the other parameters fixed. The origin of this field dependent scattering rate will be addressed below. The fits allow us to extract the cyclotron frequency as a function of field; it is exhibited by the raw spectra as the minimum in the imaginary part of the Faraday rotation. A linear fitting $\omega_c = eB/m^* = 2\pi f_c$ gives an effective mass of $0.14m_e$. By using the relation $\omega_p^2 d = \frac{n_{2D}e^2}{m^*\epsilon_0}$ and spectral weightobtained from fitting Faraday rotation, we can extract a total sheet carrier density $n_{2D} = 4.9 \pm 0.1 \times 10^{12}/\mathrm{cm}^2$. These numbers are in excellent agreement with the ones we measured at zero field, but were determined without appealing to the band structure. Note that the cyclotron resonance is primarily sensitive to high mobility channels, because in order to observe a well resolved CR $f_c \gg \Gamma$. DC transport arrives at similar conclusions. The Hall effect is linear in field (showing single channel tranport), and both it and Shubinikov-de Haas oscillations give $n_{2D} \sim 5 \times 10^{12}/\mathrm{cm}^2$, [17]. By combining these four measurements, we can conclude that $Cu_{0.02}Bi_2Se_3$ has an insulating bulk with decoupled TSSs, an E_F ~150 meV above the Dirac point and for the sample highlighted here high mobility $\mu = e/2\pi\Gamma_D m^* \sim 4000\mathrm{cm}^2/\mathrm{V}\cdot\mathrm{s}$. The features were robust to sample aging as the samples maintain an $E_F \sim 150$ meV and high mobility after sitting in air for eight months (see SI).

Films of $Cu_{0.02}Bi_2Se_3$ can be contrasted with films of pure Bi_2Se_3, which is known to have the surface chemical potential pinned at the bottom of the bulk conduction band [10, 27, 28]. In previous work we have shown that despite residual bulk conduction, TSSs dominate the transport in these MBE films [10, 21, 24]. We can use our magneto-optical THz spectroscopy to determine exactly the size of the subdominant bulk

conduction. In Fig. 2(a), we show zero field conductance spectra from a typical 100QL Bi_2Se_3 film. It has higher spectral weight than $Cu_{0.02}Bi_2Se_3$, consistent with a higher charge density. Similarly, in Fig.2(c) the plateau-like Faraday rotation at 7 Tesla at low frequencies is as large as ~0.25 radians (~ 14°) while the value for $Cu_{0.02}Bi_2Se_3$ sample is ~0.07 radians (~ 4°). $Cu_{0.02}Bi_2Se_3$ is a significant step towards quantized Faraday rotation.

In Figs. 2(b)-(d), for Bi_2Se_3, the peak in the real conductance, an edge around the inflection point in the real Faraday rotation and the dip in the imaginary Faraday rotation are exhibited at lower frequencies than in $Cu_{0.02}Bi_2Se_3$ at the same field, which indicates Bi_2Se_3 has a heavier CR mass. In Fig. 2(e), the linear fit of f_c vs. B gives an effective mass ~$0.20m_e$. We believe that this cyclotron resonance derives from TSSs, as this mass is inconsistent with the previous reported bulk effective mass $0.12m_e$ for the carrier density range $4\times10^{17}/\mathrm{cm}^3$ to $4\times10^{19}/\mathrm{cm}^3$ [29]. Moreover, the 2DEG present on some samples from band bending has an effective mass around $0.11m_e$-$0.12m_e$ [30]. Note that this value is very different than that derived in our previous work [21]. The reason for this discrepancy is discussed at length in the SI.

One can see from Fig. 2(f) that fits of the Faraday rotation using only a single Drude term are reasonably good. As before we use the spectral weight ($\omega_p^2 d = \frac{n_{2D}e^2}{m^*\epsilon_0}$) to extract a total sheet carrier density $n_{2D} \sim 1.9 \pm 0.1 \times 10^{13}/\mathrm{cm}^2$. If using Eq. 2 with the TSS dispersion, from spectral weight we find $k_F \sim 0.11\text{Å}^{-1}$, $E_F \sim 350$ meV, $n_{2D} \sim 2.0 \times 10^{13}/\mathrm{cm}^2$ and $m^* \sim 0.20m_e$, which self-consistently assigns this high mobility channel ($\mu \sim 3200 cm^2/Vs$) to TSSs. Considering that the characteristic penetration depth ($\sim \hbar v_F/\Delta$) of the TSS wavefunctions is of order 1 nm [24], ~7 ° rotation per surface is a giant rotation per unit length.

The fits to the Faraday rotation with a single Drude parameter are excellent, but significant discrepancies arise if we use the parameters determined by these fits to fit the conductance data. In Fig. 2(a), one can see that this single Drude component fit significantly underestimates the conductance by a roughly constant amount over the entire spectral range. As an E_F of ~ 350 meV corresponds to a chemical potential in the bottom of the conduction band, it is reasonable to ascribe this difference to a subdominant low mobility conduction channel coming from bulk or non-topological 2DEG. Adding this second term with a large scattering rate ($\Gamma > 4$THz) improves the conductance fit dramatically. Although the Faraday rotation is reasonably insensitive to such a low mobility channel, adding this term does improve the Faraday fits somewhat. Essentially, the second channel manifests itself as a small flat background in the Faraday rotation. For this reason we are not able to extract the effective mass of the low mobility channel. If literature values for the bulk or 2DEG mass are used, this channel has carrier density $n_{2D} \sim 8.0 \times 10^{12}/\mathrm{cm}^2$ and low mobility $\mu < 300 cm^2/Vs$. The ratio $\sigma_{TSSs}/\sigma_{total} \geqslant 90\%$ confirms that TSSs dominate transport as observed in previous THz measurements [21, 24]. This contrast further confirms $Cu_{0.02}Bi_2Se_3$ has a single TSS conduction channel.

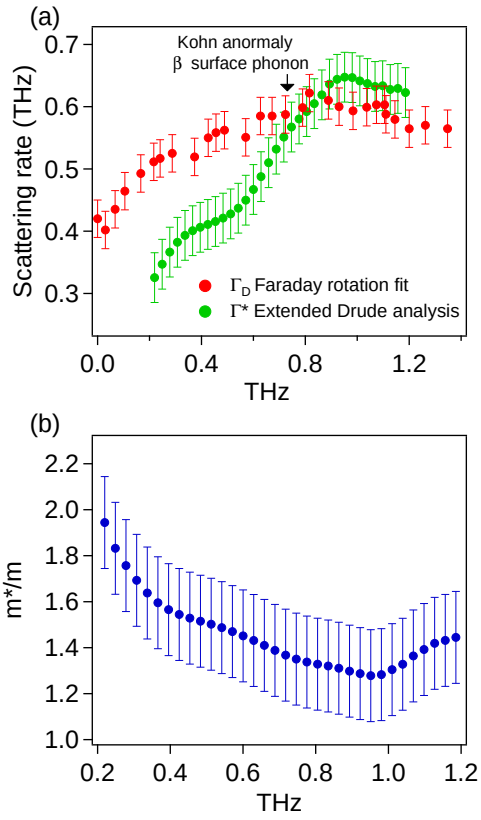

FIG. 3: (Color online) (a) Scattering rate as a function of cyclotron frequency (red). Renomalized scattering rate by mass through extended Drude analysis (green). (b) Renormalized mass as a function of frequency. The error bars express the uncertainty in ω_p.

.

Having identified the transport channels in these films and their relevant parameters, we can look in more detail at the magnetic field dependence of the scattering rates. As shown in Fig.3 the scattering rate in $Cu_{0.02}Bi_2Se_3$ has an increase with field (or cyclotron frequency), displaying a maximum near a cyclotron frequency of 0.9THz ±0.1 THz. As discussed in the SI, we can exclude magnetic field induced spin- or orbital-based electronic mechanisms for this broadening[31]. Because it is the only relevant energy scale in this range, we believe the effect is due to a coupling of electrons to phonons. Similar CR broadening has been observed in GaInAs quantum wells and graphene around phonons [32, 33]. One generally expects that the a CR will become broader at energies above the relevant phonons because new scattering channels become available.

An extended Drude model (EDM) analysis of zero field data supports the inference that the broadening is due to coupling to a low energy mode like a phonon. Such analysis allows one to quantify subtle deviations from pure Drude behavior (e.g. Lorentzian form) as shown in Fig.1(a) inset in the form of frequency dependent masses and scattering rates. In such analysis one inverts the data (where G_D is Drude intra-

band contribution to the conductance) via Eqs. (4)

$$\frac{1}{\tau(\omega)} = \frac{\omega_p^2 d}{4\pi}\mathrm{Re}(\frac{1}{G_D}), \quad \frac{m^*}{m} = -\frac{\omega_p^2 d}{4\pi\omega}\mathrm{Im}(\frac{1}{G_D}). \qquad (4)$$

An EDM analysis of the zero field conductance data shows a frequency dependent scattering ($\Gamma_D(\omega) = \frac{1}{2\pi\tau}$) and an electron-phonon coupling constant ($\lambda(\omega) = \frac{m^*}{m} - 1$). As shown in Fig.3(b), low frequency limit of $\lambda \sim 0.9 \pm 0.2$ roughly agree with previous experiments $\lambda \sim 0.43$ [34] and calculation $\lambda \sim 0.86$ [35]. Since the mass renormalization effects here are reasonably small, we approximate the bare plasma frequency with the plasma frequency extracted from zero-field conductance and CR fits.

From the EDM parameters we can define a fully renormalized scattering rate $\Gamma_D^*(\omega) = \Gamma_D(1 + \lambda(\omega))$ which will be the width of the conductance spectral features. $\Gamma^*(\omega)$ includes the renormalization effects of the lifetime as well as the mass. Plotting this quantity in Fig.3(a), we find the general trend and energy scales of the scattering rate from the EDM are the same as the width of the cyclotron resonance. The data from the extended model is a sharper version of the cyclotron resonance, which is expected because the cyclotron resonance fit is assuming a frequency independent scattering rate.

The correspondence between these two analyses shows that the magnetic field does not have a major effect on the cyclotron resonance broadening, and we propose electron-phonon coupling as cause of these effects. In the present case the energy scale of the saturation (0.9 THz) is close to scale of the previously observed Kohn anomaly of surface the β phonon, 0.75 THz at $2k_F$ [36] [37]. The energy scale also matches closely to the scale of the maximum acoustic phonon energy that can can couple to cross Fermi surface scattering $c_l \times 2k_F/2\pi \sim 0.6$ THz (where $c_l \sim 2900$m/s is longitudinal phonon velocity) [38]. We should also point out a low-energy E_{1g} phonon also exists at ~1.17THz (bulk value) and may also be relevant here. Unfortunately, it is difficult to distinguish these possibilities [36, 39, 40] without momentum resolved probes.

In conclusion, we have observed THz range cyclotron resonances from TSSs in $Cu_{0.02}Bi_2Se_3$ and Bi_2Se_3 MBE films. In $Cu_{0.02}Bi_2Se_3$, only a single high-mobility channel is necessary to fit the conductance and Faraday rotations, which is consistent with a pure TSS channel. We find that $Cu_{0.02}Bi_2Se_3$ is a true bulk-insulating topological insulator. It is stable in air for 8 months by the protection of a Se capping layer. In pure Bi_2Se_3, the high mobility TSSs dominate the Faraday rotations, but a second low mobility channel is needed to fit the zero field complex conductance. We also observe an anomalous broadening effect at higher fields in the cyclotron resonance that - supported by an extended Drude model analysis - we ascribe to coupling of electrons to phonons. The development of the true topological insulator $Cu_{0.02}Bi_2Se_3$ is a significant move towards the observation of the predicted quantized Faraday rotation and many-body interactions in these systems.

We would like to thank A. Kuzmenko, G. Refael, R. Valdes Aguilar, and S. Valenzuela for discussions. We also thank L. Pan for help drawing Fig.S1. THz measurements at JHU and film growth and development at Rutgers were supported by NSF DMR-1308142, with additional support at JHU by the Gordon and Betty Moore Foundation through Grant No. GBMF2628 to NPA.

* Electronic address: npa@pha.jhu.edu

[1] M. Z. Hasan and C. L. Kane, Rev. Mod. Phys. **82**, 3045 (2010).
[2] M. Z. Hasan and J. E. Moore, Ann. Rev. Cond. Mat. Phys. **2**, 55 (2011).
[3] X.-L. Qi and S.-C. Zhang, Rev. Mod. Phys. **83**, 1057 (2011).
[4] D. Pesin and A. H. MacDonald, Nat. Mat. **11**, 409 (2012).
[5] L. Fu and C. L. Kane, Phys. Rev. Lett. **100**, 096407 (2008).
[6] X.-L. Qi, T. L. Hughes, and S.-C. Zhang, Phys. Rev. B **78**, 195424 (2008).
[7] W.-K. Tse and A. H. MacDonald, Phys. Rev. B **82**, 161104 (2010).
[8] D. Basov, M. Fogler, A. Lanzara, F. Wang, and Y. Zhang, Reviews of Modern Physics **86**, 959 (2014).
[9] A. A. Taskin, S. Sasaki, K. Segawa, and Y. Ando, Phys. Rev. Lett. **109**, 066803 (2012).
[10] N. Bansal, Y. Kim, M. Brahleck, E. Edrey, and S. Oh, Phys. Rev. Lett. **109**, 116804 (2012).
[11] Y. S. Hor, A. Richardella, P. Roushan, Y. Xia, J. G. Checkelsky, A. Yazdani, M. Z. Hasan, N. P. Ong, and R. J. Cava, Phys. Rev. B **79**, 195208 (2009).
[12] Z. Ren, A. A. Taskin, S. Sasaki, K. Segawa, and Y. Ando, Phys. Rev. B **82**, 241306 (2010).
[13] J. Xiong, A. Petersen, D. Qu, Y. Hor, R. Cava, and N. Ong, Physica E **44**, 917 (2012).
[14] Z. Ren, A. A. Taskin, S. Sasaki, K. Segawa, and Y. Ando, Phys. Rev. B **84**, 165311 (2011).
[15] D. Kim, S. Cho, N. P. Butch, P. Syers, K. Kirshenbaum, S. Adam, J. Paglione, and M. S. Fuhrer, Nature Physics **8**, 459 (2012).
[16] Y. Xu, I. Miotkowski, C. Liu, J. Tian, H. Nam, N. Alidoust, J. Hu, C.-K. Shih, M. Z. Hasan, and Y. P. Chen, Nature Physics **10**, 956 (2014).
[17] M. Brahlek, N. Koirala, M. Salehi, N. Bansal, and S. Oh, Phys. Rev. Lett. **113**, 026801 (2014).
[18] I. Crassee, J. Levallois, A. Walter, M. Ostler, A. Bostwick, E. Rotenberg, T. Seyller, D. Van Der Marel, and A. Kuzmenko, Nature Physics **7**, 48 (2010).
[19] Z. Jiang, E. Henriksen, L. Tung, Y.-J. Wang, M. Schwartz, M. Han, P. Kim, and H. Stormer, Phys. Rev. Lett. **98**, 197403 (2007).
[20] J. Kono and N. Miura, High Magnetic Fields: Science and Technology, Volume III, World Scientific, Singapore (2006).
[21] R. Valdés Aguilar, A. V. Stier, W. Liu, L. S. Bilbro, D. K. George, N. Bansal, L. Wu, J. Cerne, A. G. Markelz, S. Oh, et al., Phys. Rev. Lett. **108**, 087403 (2012).
[22] G. S. Jenkins, D. C. Schmadel, A. B. Sushkov, H. D. Drew, M. Bichler, G. Koblmueller, M. Brahlek, N. Bansal, and S. Oh, Phys. Rev. B **87**, 155126 (2013).
[23] H. Lee, C. Xu, S. Shubeita, M. Brahlek, N. Koirala, S. Oh, and T. Gustafsson, Thin Solid Films **556**, 322 (2014).
[24] L. Wu, M. Brahlek, R. V. Aguilar, A. V. Stier, C. M. Morris,

Y. Lubashevsky, L. S. Bilbro, N. Bansal, S. Oh, and N. P. Armitage, Nature Physics **9**, 410 (2013).

[25] C. Morris, R. Valdés Aguilar, A. Stier, and N. Armitage, Optics Express **20**, 12303 (2012).

[26] $t_\pm = t_{vs}e^{i\phi_s}t_{sfv\pm}$ is the transmission for right/left hand circularly polarized light, where t_{vs} is the transmission from vacuum to substrate $t_{vs} = 2/(1+n_s)$, $t_{sfv\pm}$ is the transmission from substrate thought film then to vacuum $t_{sfv\pm} = 2n_s/(1 + n_s + Z_0G_\pm)$. $e^{i\phi_s}$ is the phase accumulation inside the substrate[41].

[27] Y. Xia, D. Qian, D. Hsieh, L. Wray, A. Pal, H. Lin, A. Bansil, D. Grauer, Y. Hor, R. Cava, et al., Nature Physics **5**, 398 (2009).

[28] D. Hsieh, Y. Xia, D. Qian, L. Wray, J. Dil, F. Meier, J. Osterwalder, L. Patthey, J. Checkelsky, N. Ong, et al., Nature **460**, 1101 (2009).

[29] H. Hohler, physica status solidi (b) **58**, 91 (1973).

[30] M. Bianchi, D. Guan, S. Bao, J. Mi, B. B. Iversen, P. D. C. King, and P. Hofmann, Nature Communications **1**, 128 (2010).

[31] In principle, the Zeeman effect and orbital effect should increase the scattering rate as well. Neverthless, Zeeman effect should be much smaller than a 50% increase at low field. Orbital effects without inter-Landau-Level (LL) coupling cannot explain the saturation behavior above 4T. Orbital effects with inter-LL coupling will lead to magneto-oscillations of transport lifetime (inverse scattering rate) above 3 T when $\omega_c\tau \geq 1$. (See SI for detailed calculation.).

[32] M. Orlita, C. Faugeras, G. Martinez, S. A. Studenikin, and P. J. Poole, EPL **92**, 37002 (2010).

[33] M. Orlita, L. Tan, M. Potemski, M. Sprinkle, C. Berger, W. de Heer, S. Louie, and G. Martinez, Phys. Rev. Lett. **108**, 247401 (2012).

[34] X. Zhu, L. Santos, C. Howard, R. Sankar, F. Chou, C. Chamon, and M. El-Batanouny, Phys. Rev. Lett. **108**, 185501 (2012).

[35] S. Giraud and R. Egger, Phys. Rev. B **83**, 245322 (2011).

[36] X. Zhu, L. Santos, R. Sankar, S. Chikara, C. Howard, F. Chou, C. Chamon, and M. El-Batanouny, Phys. Rev. Lett. **107**, 186102 (2011).

[37] Ref. [36] reported the surface β phonon has frequency ~1.8 THz and surface spring constant is 75% of the bulk value. Therefore, the surface β phonon could be a softening bulk A_{1g} Raman active phonon (2.23 THz bulk value). The surface β phonon shows a Kohn anomaly at 2 k_f with ~ 0.75THz phonon frequency.

[38] D. Kim, Q. Li, P. Syers, N. P. Butch, J. Paglione, S. D. Sarma, and M. S. Fuhrer, Phys. Rev. Lett. **109**, 166801 (2012).

[39] J. A. Sobota, S.-L. Yang, D. Leuenberger, A. F. Kemper, J. G. Analytis, I. R. Fisher, P. S. Kirchmann, T. P. Devereaux, and Z.-X. Shen, Phys. Rev. Lett. **113**, 157401 (2014).

[40] J. Qi, X. Chen, W. Yu, P. Cadden-Zimansky, D. Smirnov, N. H. Tolk, I. Miotkowski, H. Cao, Y. P. Chen, Y. Wu, et al., Applied Physics Letters **97**, 182102 (2010).

[41] J. N. Hancock, J. L. M. van Mechelen, A. B. Kuzmenko, D. van der Marel, C. Brüne, E. G. Novik, G. V. Astakhov, H. Buhmann, and L. W. Molenkamp, Phys. Rev. Lett. **107**, 136803 (2011).